Electronic Supplementary Information (ESI) for Chemical Communications

This journal is (c) The Royal Society of Chemistry

A Reversible Fluorescence Nanoswitch Based on Bifunctional Reduced Graphene Oxide: Use for Detection of Hg^{2+} and Molecular Logic-Gate Operation

Wei Tao Huang, Yan Shi, Wan Yi Xie, Hong Qun Luo*, and Nian Bing Li*

Key Laboratory of Eco-environments in Three Gorges Reservoir Region (Ministry of Education), School of Chemistry and Chemical Engineering, Southwest University, Chongqing 400715, P.R. China

1. Materials

$HgCl_2$, $Hg(NO_3)_2$, $MgCl_2$, $CaCl_2$, $Co(NO_3)_2$, Ni $(NO_3)_2$, $Cd(NO_3)_2$, $Cu(NO_3)_2$, $Cr(NO_3)_2$, $Zn(NO_3)_2$, $AgNO_3$, $MnCl_2$, $Fe_2(SO_4)_3$, and $Pb(NO_3)_2$ (analytical grade) were purchased from Sinopharm Chemical Reagent Co., Ltd., China. Cysteine and tris(hydroxymethyl)aminomethane (Tris) were purchased from Aladdin-reagent Co., China. Tris (2-carboxyethyl) phosphine (TCEP) was purchased from Sigma (St. Louis, MO). Acridine orange (AO, Fluka product) was purchased from Shanghai Chemical Co., China. Tris-HAc buffer solution (pH 7.0) contained 20 mM Tris.

AO stock solution (10 mM) was prepared by dissolving AO with doubly distilled water. Hg^{2+} stock solution (0.1 M) was prepared by dissolving $Hg(NO_3)_2$ with 0.5% HNO_3. The pH of the Hg^{2+} stock solution was adjusted to 6.0, to prevent the formation of HgO particles. The Hg^{2+} stock solution was

diluted to desired concentration with 20 mM Tris-HAc buffer (pH 7.0).

All other chemicals not mentioned here were of analytical reagent grade and were used as received. Doubly distilled water was used throughout.

2. Synthesis of reduced graphene oxide

GO was synthesized from graphite (spectral pure, Sinopharm Chemical Reagent Co., Ltd., China) by a modified Hummers method.[S1] As-synthesized GO was dispersed in water to obtain a yellow-brown aqueous solution with the aid of magnetic stirring and ultrasonication. Typically, 0.844 g of as-synthesized GO was dispersed in 1 L of doubly distilled water under the aid of magnetic stirring for 30 min, and then sonicating for 30 min at a power of about 100 W using a KQ 218 probe-type sonicator (Kunshan Ultrasonication Instrument Co., Ltd, China). The homogeneous GO dispersion had a concentration of about 0.844 mg/mL. rGO was prepared by the chemical reduction of GO with hydrazine.[S2] Fifty milliliters of the diluted homogeneous GO dispersion (0.15 mg/mL) was mixed with 10 μL of hydrazine monohydrate (80 wt% in water) and 104 μL of ammonia solution (28 wt % in water). The mixture was stirred at 95 °C for 1 h. After reduction, a black dispersion with a small amount of black precipitate was obtained. Successively, this black dispersion was filtered through glass cotton to remove the precipitate and yield a stable homogeneous dispersion of rGO. The concentration of rGO was determined to be 0.14 mg/mL.

3. Atomic force microscopy (AFM) imaging

A typical sample for AFM imaging was prepared by spotting 10 μL of a sample onto a freshly cleaved mica surface. The mica substrate was mechanically circumrotated to allow the droplet to spread well on the mica surface. The mica surface was dried with compressed air before imaging. AFM imaging was performed on a Multimode microscope (Veeco, USA) with a Nanoscope IIIa controller, equipped with a Nanoscope Quadrex in tapping mode using a TESP7 Veeco AFM tip.

4. Raman spectra measurement

The Raman spectra were obtained by a RFS100/S Bruker (Bruker Optics, Billerica, MA) NIR-FT spectrophotometer equipped with an InGaAs detector cooled by liquid nitrogen. Raman excitation at 1064 nm was provided by a Nd:YAG laser. The laser power used was 300 mW, and the spectra were accumulated for 300 scans at the resolution 4 cm^{-1}.

5. FTIR spectra measurement

Each sample for FTIR was mixed with KBr and then finely ground to make a pellet. Infrared spectroscopic measurements were performed in the range 4000–500 cm^{-1} on a Bruker Tensor 27 FTIR spectrometer (Bruker Optics, Billerica, MA).

6. X-ray photoelectron spectroscopy

A piece of freshly cut aluminum foil (cut into a 1×1 cm^2 square) was used to support 10 μL of sample solution, which was air-dried at room temperature. This sample deposition process could be repeated several times to ensure enough sample loading. The XPS measurements were carried out with an ESCALAB 250 high performance photoelectron spectrometer (Thermo VG Scientific, U.K.) with an Al Kα (1486.6 eV) radiation. All spectra obtained were calibrated to a C1s peak at 284.6 eV, and fitted by Avantage (a freeware).

7. Fluorescence emission and UV-visible absorption spectra measurements

Fluorescence emission spectra were recorded on a Hitachi F-4500 fluorescence spectrophotometer (Tokyo, Japan); excitation wavelength: 490 nm; emission wavelength: 540 nm; slit: 10 nm; PMT voltage: 400 V. UV-visible absorption spectra were recorded on a Shimadzu UV-visible spectrophotometer (Suzhou Shimadzu Instrument Co., Ltd., China).

8. Characterization of GO and rGO.

As shown in Figure S1, The average thickness of as-made rGO sheets was measured to be approximately 1 nm; The diluted solution of GO was yellow brown, whereas that of rGO was black. A successful reduction of GO to rGO by hydrazine was verified by monitoring the absorption spectra of the samples: the absorption peak at 230 nm, characteristic of GO, shifted to 268 nm (typical for rGO).[S3] Fluorescence spectra provided that GO has weak autofluorescence in visible range, whereas the corresponding rGO is essentially not fluorescent at all. X-ray photoelectron spectroscopic (XPS) data provided further information for the GO-to-rGO conversion, according to the diminished C-O and C=O content.

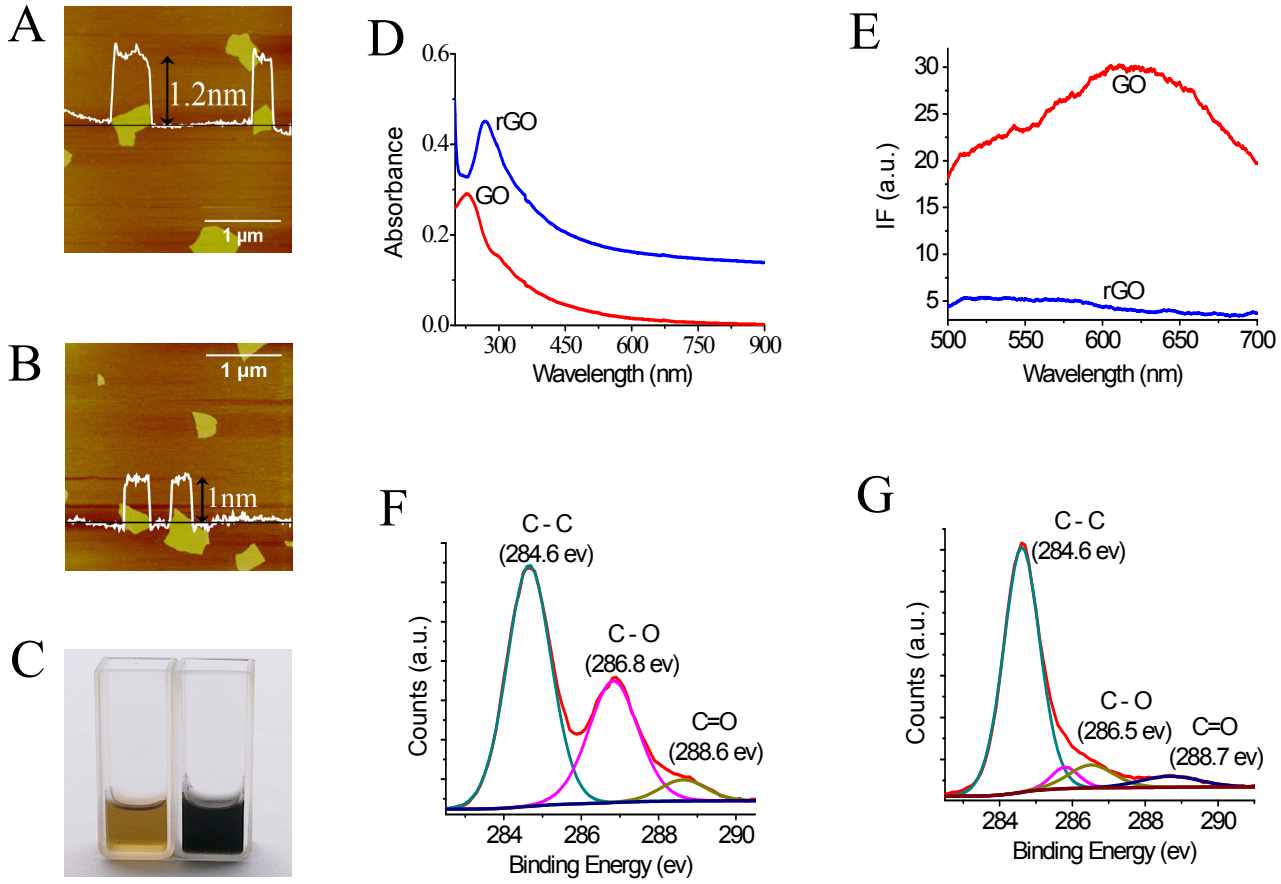

Fig. S1 AFM images and height analyses of (A) GO and (B) rGO. (C) Photography of GO (left) and rGO (right). The optical absorbance (D) and fluorescence spectra (E) of GO and rGO sheets dispersed in water upon excitation at 400 nm, PMT = 700 V. XPS analyses of samples; C1s XPS profiles of (F) GO and (G) hydrazine reduced rGO.

Raman spectroscopy is a useful tool for identifying carbon materials. Fig. S2 shows the Raman spectra of GO and rGO. GO and rGO both display two prominent peaks at 1602 and 1300 cm^{-1} corresponding to the G and D bands, respectively.[S4] Although these bands still exist in the Raman spectrum of rGO, the D/G intensity ratio increases compared with that of GO, thus indicating the successful reduction of GO.[S5] FTIR spectra (Fig. S3) can give a qualitative measure of the deoxygenating reactions. The spectrum of the GO showed a rich collection of transmission bands corresponding to -OH stretching vibrations from both water and GO (around 3446 cm^{-1}), carboxylic acid (1630-1730 cm^{-1}), the -OH attached to the aromatic carbon backbone (1300-1400 cm^{-1}), C–O stretching vibration (around 1134 cm^{-1}) and epoxide groups (around 1110 cm^{-1}).[S6] After the chemical reduction, the peaks for oxygen functional groups were reduced significantly, indicating that the reduction of GO was successful. The spectra of rGO around 3446 cm^{-1} can be assigned to O-H stretching vibrations from water.[S6a]

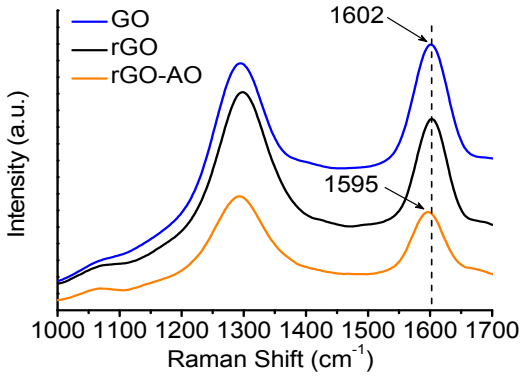

Fig. S2 Raman spectra of GO, rGO, and rGO-AO.

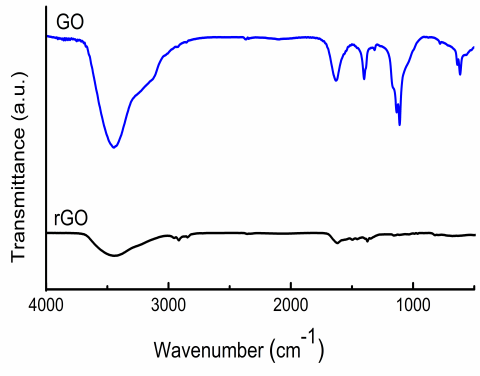

Fig. S3 FTIR spectra of GO and rGO.

9. Comparison of the fluorescence quenching abilities between GO and rGO

We investigated the quenching ability of GO to the fluorescence of AO and the results are shown in Fig. S4. It can be seen from Fig. S4 A, B, and C that the fluorescence of AO (1 μM) titrated with GO and rGO both becomes significantly reduced. The results suggest that both GO and rGO can efficiently quench the fluorescence of AO dyes, and the fluorescence quenching ability of AO depends on the concentrations of GO and rGO. By comparison, the fluorescence quenching of GO (14.52 μg/mL) is close to that of rGO (2.07 μg/mL), in which the concentration of GO is about seventimes that of rGO. As shown in Fig. S4 D, upon the addition of equal amount (around 2.1

μg/mL) of GO and rGO, nearly 98.6% fluorescence quenching was observed for the rGO-AO complex, whereas only 41.4% fluorescence quenching was observed for the GO-AO complex. Thus, it suggests that the fluorescence quenching ability of rGO is stronger than that of GO.[S7] The strong quenching by GO is likely due to the residual sp^2 graphitic domains in the basal plane that survived the severe chemical oxidation.[S8] In a similar manner, quenching of nearby fluorescent dyes by rGO can attribute to the sp^2 domains within rGO.[S7] As shown in Figs. S1, S2, and S3, the oxygen functional groups of GO sheets have been removed after reduction, resulting in the ratio of sp^2 to sp^3 domains of the rGO sheets higher than that of the GO sheets, which further enhances π–π stacking interactions between fluorescent dye (AO) and the aromatic regions of rGO. Thus, the quenching ability of rGO is better than that of GO.

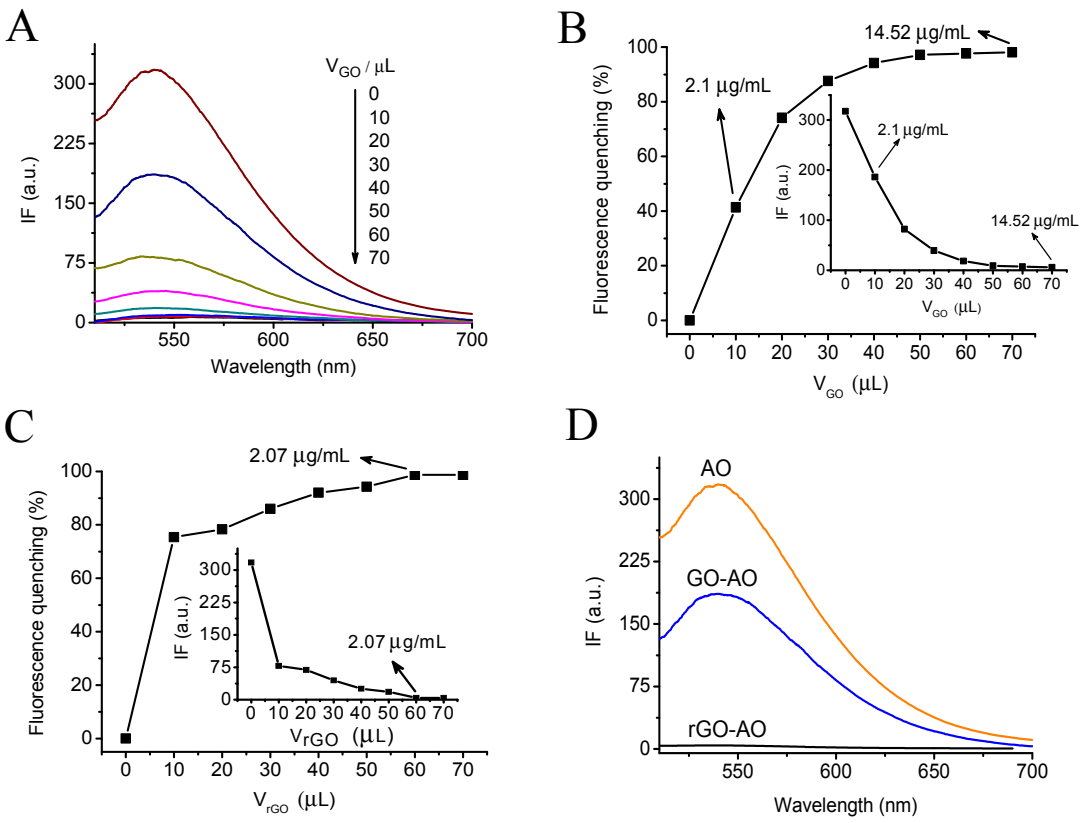

Fig. S4 (A) Fluorescence emission spectra recorded during the process of titration of 4.0 mL of 1 μM AO aqueous solution with various volumes of 0.844 mg/mL GO dispersion. (B) Dependence of fluorescence quenching (%) of AO as a function of V_{GO} used for titration. Inset: Dependence of fluorescence intensity of AO as a function of V_{GO}. (C) Dependence of fluorescence quenching (%) of AO as a function of V_{rGO}. Inset: Dependence of fluorescence intensity of AO as a function of V_{rGO}. (D) Fluorescence emission spectra of AO (1 μM), GO-AO, and rGO-AO, upon the addition of equal amount (around 2.1 μg/mL) of GO and rGO. Excitation wavelength: 490 nm; emission wavelength: 540 nm. Buffer: 20 mM Tris-HAc solution, pH 7.0.

10. Characterization of the rGO-AO complex

We investigated the change in absorption spectrum for the interaction between rGO and AO. As shown in Fig. S5 A, The spectrum of the aqueous solution of monomeric AO features an intense absorption band at 490 and 268 nm.[S9] During the rGO titration process, we found that the absorption band of monomeric AO gradually shifted to longer wavelength. The absorption band of the rGO-AO complex formed at the end point of titration exhibited a large bathochromic shift (18 nm). Besides, we could observe that the color of the resulting rGO-AO solution became dark (Fig. S5 B, inset). We further analyzed this phenomenon of bathochromic shift. Although the protonation of AO, polarizability of environment, and solvent effect[S10] can also result in bathochromic shift, the bathochromic shifts hardly reach 18 nm. In addition, the absorption spectrum of an AO solid film deposited on a glass slide was recorded for comparison. The band of the solid film showed a 21-nm blue-shift due to H-aggregation of AO molecules (Fig. S5 B).[S10b] Thus, one reason can reasonably attribute the large bathochromic shift of the absorption band to the flattening of AO molecules caused by twist of their cationic dimethylamino.[S11] It suggests that AO can interact with rGO, resulting in the formation of rGO-AO complex.

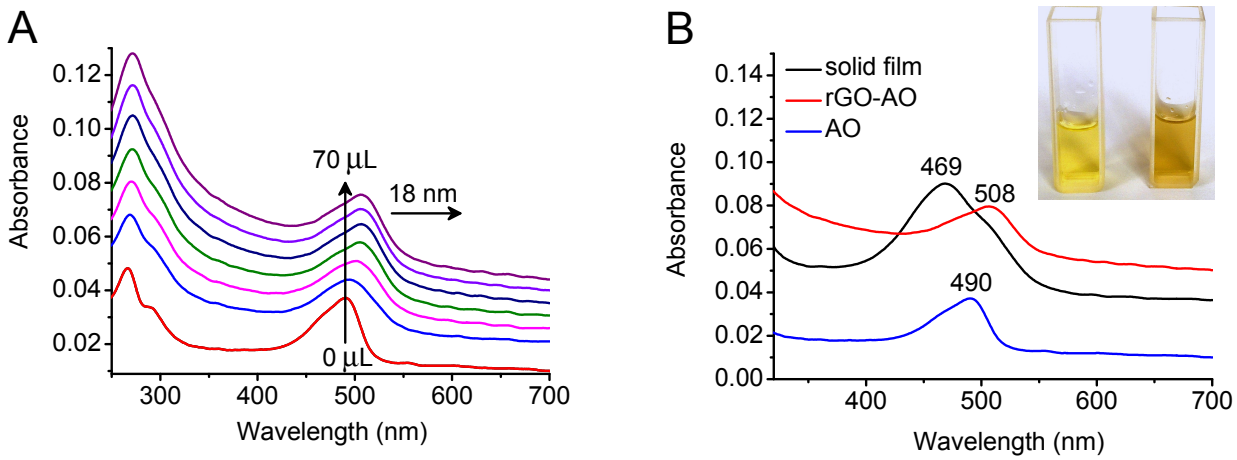

Fig. S5 (A) Absorption spectra recorded during the process of titration of 3.0 mL of 1 µM AO aqueous solution with various volumes of 0.14 µg/mL rGO dispersion. (B) Absorption spectra of monomeric AO solution (1 µM), solid-film-AO and rGO-AO complex formed at the end point of titration. Inset: photography of 10 µM AO (left) and tenfold concentration rGO-AO complex (right).

We further investigated Raman spectra of rGO-AO. Fig. S2 shows the Raman spectra of GO, rGO, and rGO-AO. By comparing the G-bands of GO, rGO, and rGO–AO, it is clear that G-band of rGO–AO occurs at 1595 cm^{-1}, which is downshifted by 7 cm^{-1} compared with that of GO and rGO. The Raman shifts of the G band for rGO–AO provide evidence for the charge transfer between the rGO sheets and AO, which suggests a strong interaction between the AO and the rGO sheet. [S12]

In addition, the evidence of interaction between rGO and AO is provided by the FTIR spectra shown in Fig. S6. The spectrum of the AO shows a rich collection of transmission bands corresponding to around 1637 (Ar: aromatic backbone)[S13], around 1594 (C=N)[S6c], and 1500-1200 cm^{-1} (C-N)[S14], respectively. The spectrum of the rGO shows few transmission bands in the range 1800-1000 cm−1, which can be assigned to aromatic backbone stretching vibration at 1625 cm^{-1}. By comparing the FTIR spectra of AO, rGO, and rGO–AO, it is clear that the spectrum of rGO-AO shows a rich collection of transmission bands corresponding to aromatic backbone stretching vibration of AO and rGO (1640-1618 cm^{-1}), C=N stretching vibration (around 1577 cm^{-1}), and C-N stretching vibration (1500-1200 cm^{-1}), respectively. The FTIR results suggest that the AO can interact with rGO and the rGO-AO complex has successfully been formed.

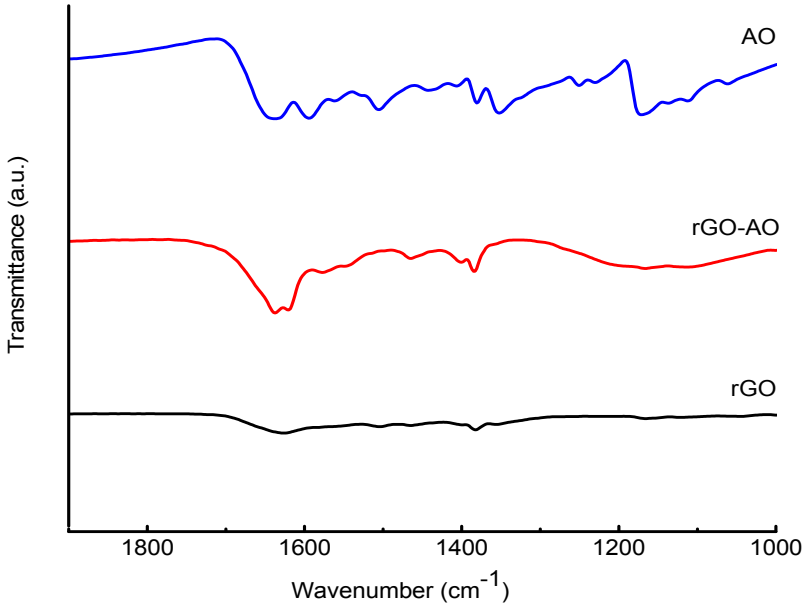

Fig. S6 FTIR spectra of AO, rGO, and rGO-AO.

11. UV-visible absorption spectra measurements for investigating the interaction between Hg^{2+} and AO

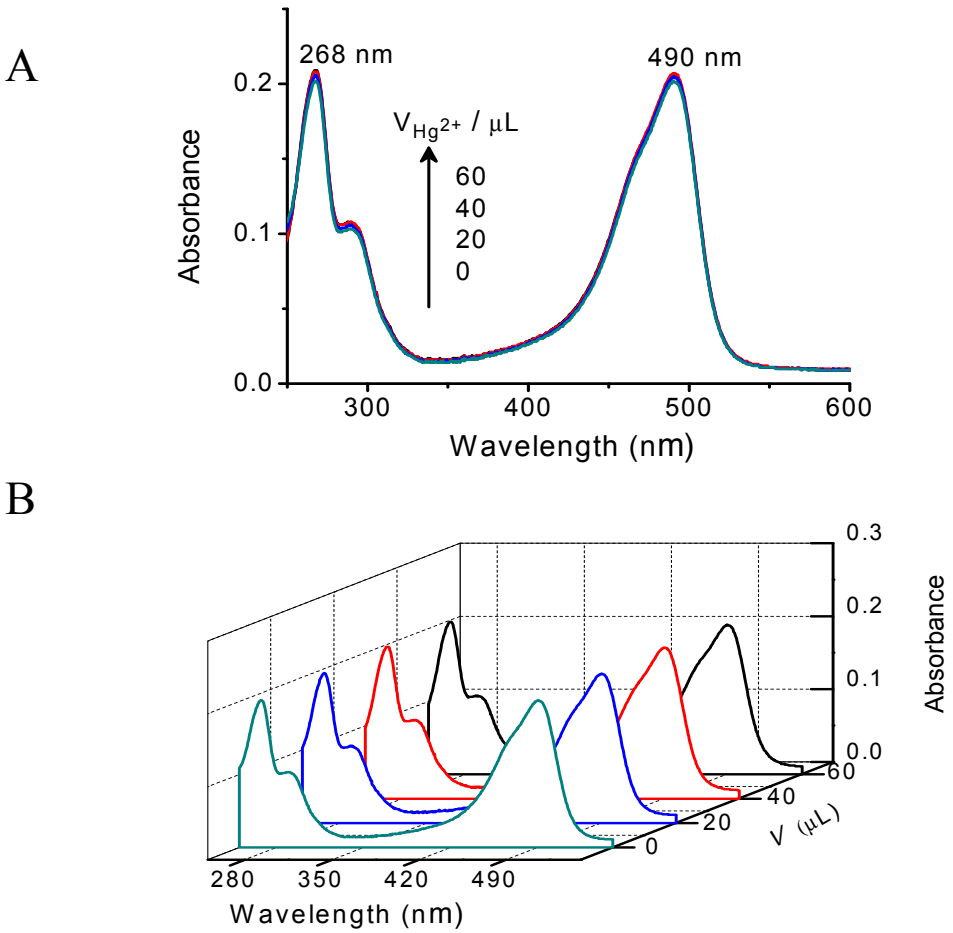

Fig. S7 (A) UV-visible absorption spectra obtained by measuring the mixtures of 3.0 mL of AO aqueous solution containing 10 μM AO and 20 mM Tris-acetic acid (pH 7.0) with different volumes of 10 mM Hg^{2+} at room temperature. (B) 3D waterfall of UV-visible absorption spectra of AO with Hg^{2+}.

12. Investigation the effect of pH on the fluorescence intensity of the rGO-AO complex and kinetic behaviors of Hg^{2+} and rGO-AO complex

The response of rGO -AO interaction at different pH values was studied. The AO was employed to test adsorption behavior upon incubated with rGO in the buffer of 20 mM Tris-HAc. The pH values of the reaction buffer were adjusted by 6 mol/L HCl and 6 mol/L NaOH solutions. A series of AO solutions with the same concentration were incubated with 2 μg/mL rGO in the buffer with different pH values for 5 min at room temperature with gentle shaking. After that, fluorescence emission spectra were obtained by measuring the mixtures. The experimental results are shown in Fig. S8 A. pH 7.0 was selected in this work.

We studied the kinetic behaviors of Hg^{2+} and rGO-AO complex by monitoring the fluorescence intensity as a function of time. Figure S8 B shows the reaction of fluorescence restoreation of AO in the presence of Hg^{2+}can be completed within 120 min.

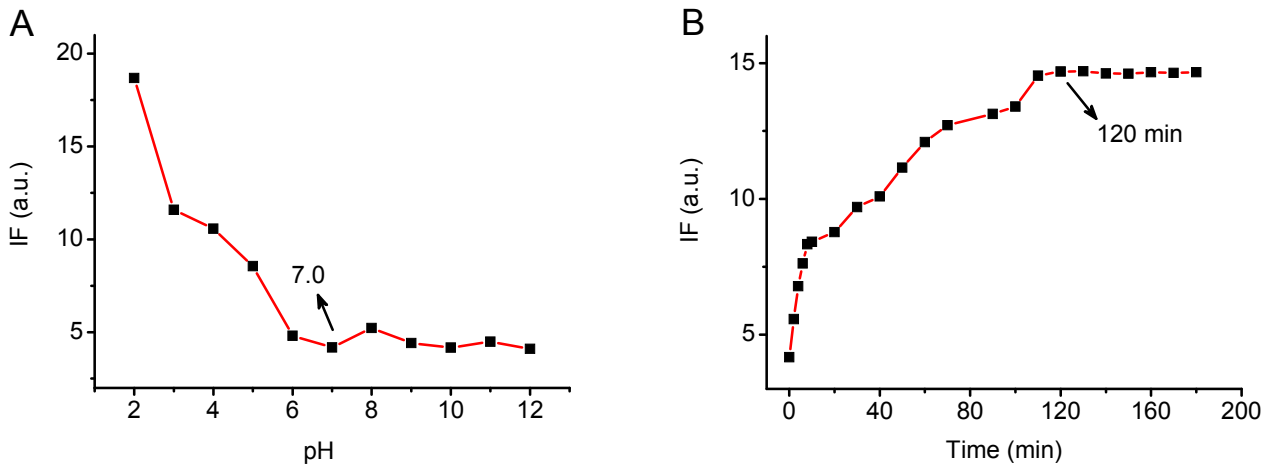

Fig. S8 (A) Fluorescence intensities of rGO-AO complex recorded in different pH ranges from 2.0 to 12.0. (B) Fluorescence restoration of rGO-AO complex as a function of incubation time after addition of 100 μM Hg^{2+} at pH 7.0.

13. Investigation of the mechanism of fluorescence quenching in the rGO-AO-Hg^{2+} system caused by the addition of Cys

Upon addition of Hg^{2+}, the fluorescence of rGO-AO can be restored; then upon addition of Cys, the fluorescence of the rGO-AO restored by Hg^{2+} can also be requenched. We presume that this phenomenon maybe occur through two routes: (1) upon addition of Cys, as a strong binder of Hg^{2+}, Cys can firstly interact with Hg^{2+} and neutralize its activity,[S15] resulting in the fluorescence quenching of AO caused by Cys-Hg^{2+} complexes, and (2) upon addition of Cys, Hg^{2+} can be strongly bound and removed from the rGO surface, resulting in the AO readsorbing on the rGO surface, re-formation of rGO-AO nanocomplex, and requenching of the dye fluorescence. To investigate the effect of Cys on AO fluorescence in the presence of Hg^{2+}, we firstly added Hg^{2+} ions into the AO solution. The fluorescence of AO dyes can be quenched by Hg^{2+} (Fig. 2B, curve b in the manuscript) because of the quenching effect of metal ions.[S16] Upon addition of Cys (activated by TCEP), the fluorescence of AO-Hg^{2+} mixture was not further quenched (Fig. 2B, curve c in the manuscript). Thus, mechanism (1) mentioned above can be ruled out. As shown in Fig. 3 D in the manuscript, the reversibility of rGO-AO nanoswitch with alternating addition of Hg^{2+} and Cys can further prove our proposed hypothesis. Thus, the dominant mechanism can be reasonably attributed to that upon addition of Cys, Hg^{2+} can be strongly bound and removed from the rGO surface, resulting in the AO readsorbing on the rGO surface, re-formation of rGO-AO nanocomplex, and requenching of the dye fluorescence.

14. Construction of fluorescent nanoswitch and operation of an INHIBIT logic gate

The rGO-AO complex was prepared by titrating with rGO (0.14 mg/mL) to AO solution (containing: 1 μM AO; 20 mM Tris-acetic acid, pH 7.0) till the fluorescence of AO was almost quenched completely and the fluorescence intensity of the resulting solution should be stable for 5 min at room temperature. After that, a suitable amount of Hg^{2+} solution was added to the rGO-AO complex solution and the fluorescence intensity of the resulting solution was recorded after 120 min incubation time.

Successively, the mixture was incubated with Cys activated by tris (2-carboxyethyl) phosphine for 5 min and then used for the determination of fluorescence.

Supplementary references

S1 W. S. Hummers, R. E. Offeman, *J. Am. Chem. Soc.*, 1958, **80**, 1339.

S2 D. Li, M. B. Muller, S. Gilje, R. B. Kaner, G. G. Wallace, *Nat. Nanotechnol.*, 2008, **3**, 101.

S3 (a) B. S. Kong, J. X. Geng, H. T. Jung, *Chem. Commun.*, 2009, 2174; (b) J. Kima, F. Kima, J. X. Huang, *Materialstoday*, 2010, **3**, 28.

S4 X. Wang, L. J. Zhi, K. Müllen, *Nano Lett.*, 2008, **8**, 323.

S5 S. Stankovich, D. A. Dikin, R. D. Piner, K. A. Kohlhaas, A. Kleinhammes, Y. Y. Jia, Y. Wu, S. T. Nguyen, R. S. Ruoff, *Carbon*, 2007, **45**, 1558.

S6 (a) H. K. Jeong, Y. P. Lee, R. J. W. E. Lahaye, M. H. Park, K. H. An, I. J. Kim, C. W. Yang, C. Y. Park, R. S. Ruoff, Y. H. Lee, *J. Am. Chem. Soc.*, 2008, **130**, 1362; (b) L. J. Cote, R. Cruz-Silva, J. X. Huang, *J. Am. Chem. Soc.*, 2009, **131**, 11027; (c) X. Z. Tang, W. J. Li, Z. Z. Yu, M. A. Rafiee, J. Rafiee, F. Yavari, N. Koratkar, *Carbon*, 2011, **49**, 1258.

S7 (a) J. Kim, F. Kim, J. X. Huang, *Mater. Today*, 2010, **3**, 28. (b) J. Kim, L. J. Cote, F. Kim, J. X. Huang, *J. Am. Chem. Soc.*, 2010, **132**, 260; (c) K. P. Loh, Q. L. Bao, G. Eda, M. Chhowalla, *Nat. Chem.*, 2010, **2**, 1015.

S8 (a) T. Nakajima, A. Mabuchi, R. Hagiwara, *Carbon*, 1988, **26**, 357; (b) A. Lerf, H. Y. He, M. Forster, J. Klinowski, *J. Phys. Chem. B*, 1998, **102**, 4477; (c) W. W. Cai, R. D. Piner, F. J. Stadermann, S. Park, M. A. Shaibat, Y. Ishii, D. X. Yang, A. Velamakanni, S. J. An, M. Stoller, J. H. An, D. M. Chen, R. S. Ruoff, *Science*, 2008, **321**, 1815.

S9 N. F. Ferreyra, G. A. Rivas, *Electroanalysis*, 2009, **21**, 1665.

S10 (a) M. Shaikh, J. Mohanty, P. K. Singh, W. M. Nau, H. Pal, *Photochem. Photobiol. Sci.*, 2008, **7**, 408; (b) J. S. Liu, N. Jiang, J. Ma, X. Z. Du, *Eur. J. Org. Chem.*, 2009, 4931; (c) A. K. Shaw, S. K. Pal, *J. Phys. Chem. B*, 2007, **111**, 4189.

S11 Y. X. Xu, L. Zhao, H. Bai, W. J. Hong, C. Li, G. Q. Shi, *J. Am. Chem. Soc.*, 2009**, 131**, 13490; (b) Z. Chernia, D. Gill, *Langmuir*, 1999, **15**, 1625.

S12 Y. Li, X. Li, C. K. Dong , J. Y. Qi, X. J. Han, *Carbon*, 2010, **48**, 3427.

S13 (a) M. A. Munawar, P. W. Groundwater, *Bull. Korean Chem. Soc.*, 1999, **20**, 456; (b) T. Ramanathan, F. T. Fisher, R. S. Ruoff, L. C. Brinson, *Chem. Mater.*, 2005, **17**, 1290.

S14 Y. Lin, J. Jin, M. Song, *J. Mater. Chem.*, 2011, **21**, 3455.

S15 W. Stricks, I. M. Kolthoff, *J. Am. Chem. Soc.*, 1953, **75**, 5673.

S16 N. Rupcich, W. Chiuman, R. Nutiu, S. Mei, K. K. Flora, Y. F. Li, J. D. Brennan, *J. Am. Chem. Soc.* 2006, **128**, 780.